Influence of the Coordination Surrounding of Co(II)- and Co(III)-Tetraphenylporphyrins on Their Destruction Processes in the Presence of Organic Peroxides

G. M. Mamardashvili[a], O. R. Simonova[a]*, N. V. Chizhova[a], and N. Zh. Mamardashvili[a]

[a] *Krestov Institute of Solution Chemistry, Russian Academy of Sciences, ul. Akademicheskaya 1, Ivanovo, 153045 Russia*
*e-mail: ors@isc-ras.ru

Abstract—The interaction of Co(II)- and Co(III)-5,10,15,20-tetraphenylporphyrins with *tert*-butylhydroxy-peroxide and di-*tert*-butylhydroxyperoxide in benzene at 298 K were studied by spectrophotometry and ^{1}H NMR spectroscopy. Kinetic parameters of the destruction reactions of porphyrin macrocycle depending on the nature of peroxide the valence of cobalt cation, and the presence and nature of axial ligands were calculated. Products of consecutive decomposition of tetrapyrrole macrocycle to monopyrroles were determined by mass spectrometry.

Keywords: Co-tetraphenylporphyrins, variable valence, organic peroxides, destruction of molecules

DOI: 10.1134/S107036321806018X

The most important property of any chemical compound is its resistance to destruction (thermal, chemical, and photochemical stability). Porphyrin molecules are known to be very stable compounds due to the presence of an extended aromatic conjugated π-system. However, in the presence of atmospheric oxygen, H_2O_2, and other redox reagents they can be subjected to destruction processes, whose rate increases with the temperature growth. The investigation into destruction of aromatic tetrapyrroles in the presence of reactive oxygen intermediates is relevant both to a better understanding of the mechanisms of catalytic and enzymatic processes occurring in the nature [1–3], and to the development of new photosensitizer types for medical purposes [4, 5]. The variety of reactive oxygen intermediates (e.g., H_2O_2, O_2^-, $ROO^•$, $HOO^•$, $OH^•$, etc.) formed as a result of photosensitized conversions of ordinary molecular oxygen leads to oxidative destruction both of the structural elements of the tumor tissue and of the photosensitizers themselves used in photodynamic therapy. However, the mechanisms of such destruction often remain unclear and controversial. The same is also true for the mechanisms of destruction of chlorophyll molecules in the aging leaves of plants and catabolism of blood heme [6–11].

A series of research on photochemically initiated decomposition of metalloporphyrin and phthalo-cyanine macrocycles in the presence of peroxides demonstrated that the photochemical destruction of aromatic tetrapyrroles strongly depends on the nature of the solvent, macrocycle, and metal cation in the macrocycle coordination site [3, 12–19]. The stability of cobalt porphyrinates in the presence of reactive oxygen is of particular concern, since porphyrinates of metal capable of variable valence are widely used as catalysts for many chemical reactions [20–23].

This work consists in the investigation of the effect of the oxidation state of the metal cation of the metal-porphyrin reaction site and its coordination sur-rounding on the interaction of cobalt-5,10,15,20-tetraphenylporphyrin with di-*tert*-butylperoxide (DBP) and *tert*-butylhydroperoxide (BHP) in benzene. The goal is to investigate the mechanisms of the destruction of tetrapyrrole macrocyclic compounds in the presence of peroxide compounds and to identify conditions that increase the resistance of Co(II,III)-porphyrins to photooxidation.

Co(II,III)-Tetraphenylporphyrins. The cobalt cation in the porphyrin macrocycle can be in the oxidation state of 2+ or 3+. The solutions of the four-coordinated

Table 1. EAS data for Co-tetraphenylporphyrins

Co	Axial ligands		Solvent	λ_{max}, nm (log ε)	References
Co(II)	–		THF–H₂O (8 : 2)	415, 529	[27]
	–		CH₂Cl₂	414, 527	[31]
	–		Benzene	414 (5.37), 528 (4.24)	
Co(II)	NO₂	–	Toluene	419, 530	[28]
	NO₂	–	CH₃OH	417	[29]
Co(III)	Cl⁻	–	CH₃OH	425.5, 541, 575	[30]
	Cl⁻	–	CH₃OH	427.4 (4.83), 541, 575	[31]
	HBP	–	CH₂Cl₂ (235 K)	427, 540	[32]
	Br⁻	–	Benzene	428, 542	
	NO₂	Py	CH₃OH	436	[29]
	NO₂	2ClPy	CH₃OH	431	[29]
	NO₂	Pip	CCl₄	435, 550, 582	[28]
	NO₂	DMS	CCl₄	439, 551, 588	[28]
	NO₂	THT	CCl₄	440, 552, 591	[28]
	CN⁻	H₂O	CH₂Cl₂	433 (5.14), 548 (4.14), 582 (3.95)	[25]
	SCN⁻	SCN⁻	THF–H₂O (8 : 2)	442	[27]
	Br⁻	CH₃OH	Benzene	435 (5.37), 549 (4.11)	
	Im	Im	Benzene	440 (5.43), 555 (4.13)	

Co(II)-5,10,15,20-tetraphenylporphyrin **1** formed through the reaction of the corresponding porphyrin ligand with Co(II) salts are stable in aprotic nonpolar solvents. Complex **1** is paramagnetic (has a $3d^7$ configuration). In the ¹H NMR spectra of this low-spin complex the signals of β-pyrrole protons and *ortho*-protons are located at 16.05 and 13.20 ppm, respectively, while the *meta*- and *para*-proton signals are at 9.91 and 9.72 ppm [24, 25].

The addition of oxidants in organic solvents to a solution of complex **1** at room temperature results in the oxidation of Co(II) to Co(III), thus giving rise to five- or six-coordinated Co(III)-5,10,15,20-tetraphenylporphyrin **2** with one or two acido and/or molecular ligands, which can be represented by various anions, organic bases, water molecules, alcohols, or gases (e.g., O₂, CO, NO, etc.) [26–32]. In the ¹H NMR spectra of diamagnetic Co(III)-tetraphenylporphyrin ($3d^6$ configuration), regardless of the nature of the axial ligands, all the proton signals are shifted upfield as compared to complex **1**, while the absorption bands in the electron absorption spectrum (EAS) are shifted to the long-wave region. According to the literature data [30–32], the Soret band of five-coordinated Co(III)-tetraporphyrins is in the range of 425–428 nm, depending on the acidoligand and solvent, while that of six-coordinated complexes is shifted to an even longer wavelength region, up to 433–442 nm (Table 1).

In the present work, Co(II)-tetraphenylporphyrin **1** and Co(III)-tetraphenylporphyrins, like five-coordinated complex **2a** [specifically, Co(III)(Br)-tetraphenylporphyrin], six-coordinated complex **2b** [Co(III)(Br)·CH₃OH-tetraphenylporphyrin], and six-coordinated diaxial complex with imidazole **2c** (Co(III)-diimidazole tetraphenylporphyrin), were studied. Complex **2c** was prepared by two methods (Scheme 1).

The formation of **2c** from **2b** was monitored spectrophotometrically (Fig. 1). This thermodynamic process occurs in two steps. In the first step characterized by the red shift of the absorption bands in the EAS at small concentrations of imidazole, a methanol molecule is replaced with an imidazole molecule [Eq. (1)]. The Soret band in this case is shifted by 8 nm (436 nm → 445 nm). In the second step, the bromine atom is replaced with the second imidazole molecule under the imidazole excess conditions [Eq. (2)], which is accompanied by a short-wavelength shift of the absorption bands in the EAS (445 nm → 440 nm).
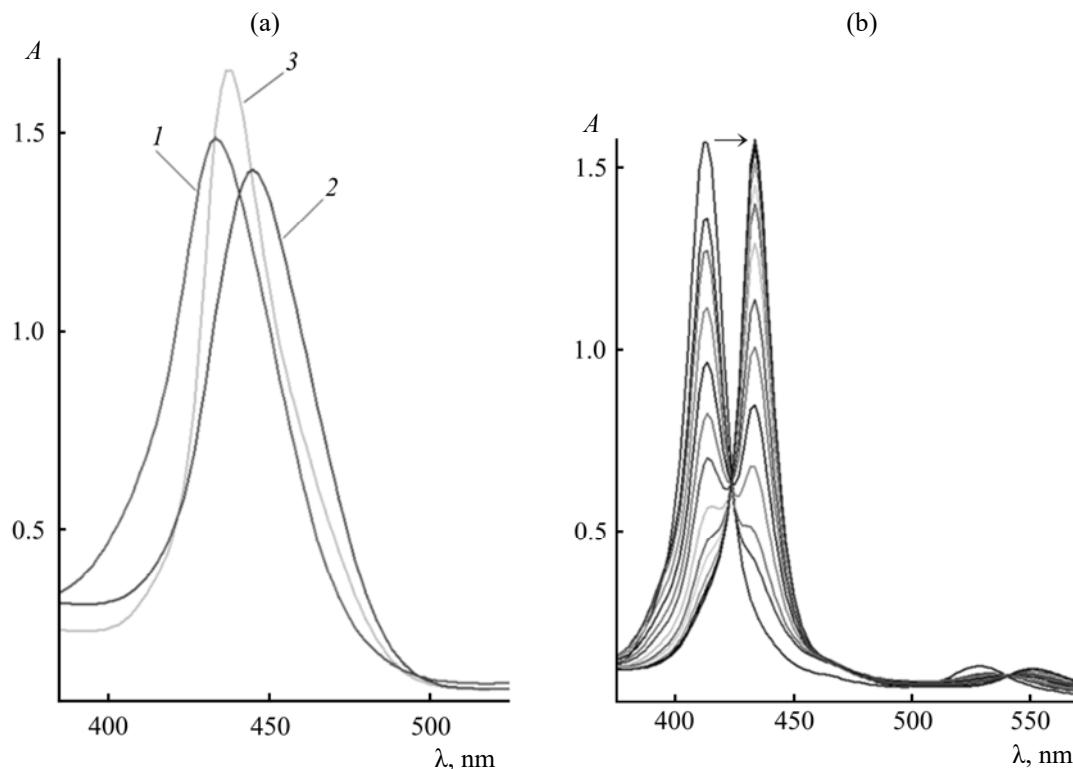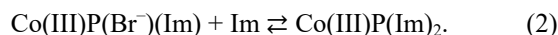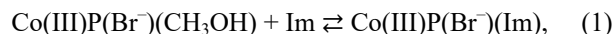
Fig. 1. Changes in the ESP observed during spectrophotometric titration of compound **2b** with (a) imidazole and (b) spectral changes observed in the interaction of complex **1** with imidazole in time in benzene at 298 K. (*1*) Co(III)P(Br), (*2*) Co(III)P(Br)(Im), and (*3*) Co(III)P(Im)$_2$.

$$Co(III)P(Br^-)(CH_3OH) + Im \rightleftarrows Co(III)P(Br^-)(Im), \quad (1)$$

$$Co(III)P(Br^-)(Im) + Im \rightleftarrows Co(III)P(Im)_2. \quad (2)$$

The preparation of **2c** from compound **1** involves oxidation of the cobalt cation to Co(III) occurring over time [Eqs. (3), (4)] [28]. The reaction products [Eqs. (2) and (4)] are identical.

$$Co(II)P + Im \rightleftarrows Co(II)P(Im), \quad (3)$$

$$Co(II)P(Im) + Im + [O] \rightarrow Co(II)P(Im)_2. \quad (4)$$
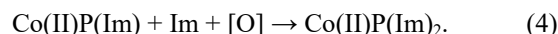
Interaction of Co(II)P and Co(III)P with peroxides. The interactions of complex **1** with various hydroxyperoxides at low temperatures were studied in [32]. Those studies demonstrated that at 233 K such interaction results in the oxidation of Co^{2+} to Co^{3+} and the formation of monoaxial complex $Co^{III}P(L)$ **2d** (Scheme 2).

Our investigations have shown that, at room temperature, reactions of all the four examined Co-porphyrins (**1**, **2a–2c**) with di-*tert*-butyl peroxide and *tert*-butylhydroxyperoxide in benzene are accompanied by destruction of the tetrapyrrole porphyrin macrocycle leading to a complete discoloration of working solutions. Analysis of the changes in the electron

absorption spectra observed in the course of the reaction of complex **1** with peroxides (Figs. 1, 2) indicates the occurrence of two processes in the reaction system (Table 2). The first process is the oxidation of the Co(II) central cation in porphyrinate **1** to Co(III) [Eq. (5)].

$$1 + ROOR' \rightarrow 3a. \quad (5)$$

The distinct red shifts of the absorption bands in the EAS, as well as the appearance of proton signals in the ^1H NMR spectral region corresponding to Co(III) complexes, clearly evidence that intermediate **3a** formed by reaction (5) is the Co(III) complex of tetraphenylporphyrin (Fig. 2).

The EAS of intermediate **3a** (437 and 548 nm) suggests that this compound is a six-coordinated Co(III)-tetraphenylporphyrin with two axially coordinated additional ligands.
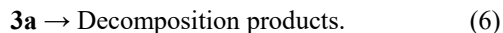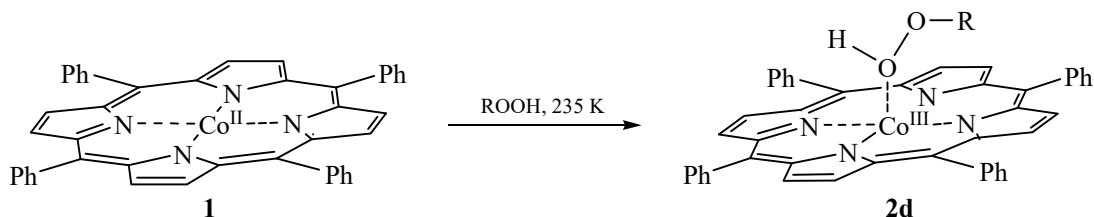
The second spectrally recorded process occurring during the reaction of complex **1** with peroxides is the destruction of the porphyrinate macrocycle proper [Eq. (6)], accompanied by a decrease in the intensity of the absorption bands at 436 and 548 nm (Fig. 2a).

Scheme 1.

B – organic base.

Scheme 2.

$$3a \rightarrow \text{Decomposition products.} \qquad (6)$$
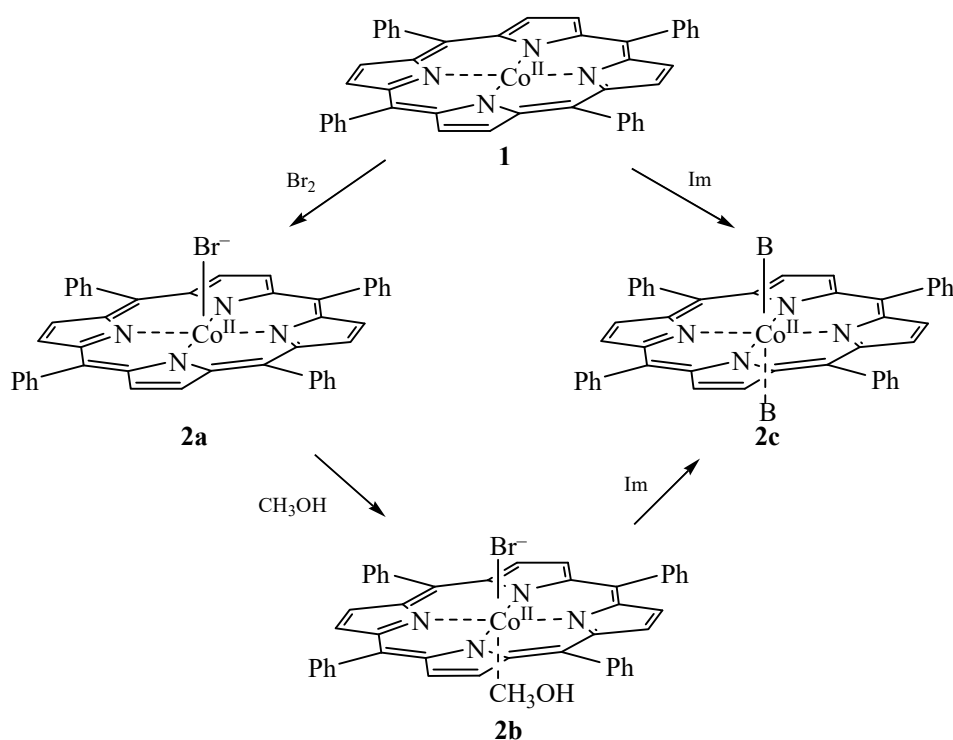
Since the macrocycle destruction proceeds concurrently with the oxidation of the cobalt cation, the band intensity at 436 nm begins to decline before reaching its maximum.

The rates of both processes {oxidation [Eq. (5)] and destruction [Eq. (6)], Table 2} and their ratio (k_1/k_2) depend both on the concentration of peroxide and its nature. The larger the ratio k_1/k_2, the higher the intensity maximum attainable by the band at 436 nm and the easier it is to distinguish these processes. The benzene solution of complex **1** in the presence of hydroperoxide is almost completely discolored in 2 h, while the same takes one day in the ROOR case.

In the interaction of Co(III)-tetraphenylporphyrins **2a–2c** with peroxides ROOR and ROOH, the valence

of the cobalt cation does not change (Scheme 3). Addition of both investigated peroxides to benzene solutions of Co(III)-porphyrins reduces the intensity of the bands in the EAS (Fig. 3). Moreover, if the Soret band in the **2a** and **2b** spectra (λ_{max} 428, 435 nm) suffers red shif (up to 437 nm) with the fall in intensity, the corresponding bands for **2c** are shifted blue (from 440 to 437 nm), which implies that, for Co(III)-porphyrinates with different coordination surrounding, the decomposition intermediate is **3b** [Eq. (7)], whose EAS shows a maximum in the 437 nm region.

$$\mathbf{2a–2c} \rightarrow \mathbf{3b} \rightarrow \text{Decomposition products.} \qquad (7)$$
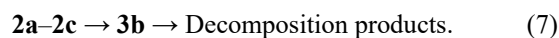
The most likely structure of intermediates **3a** and **3b** is six-coordinated Co(III)-tetraphenylporphyrin, wherein one of the axial ligands is a peroxide
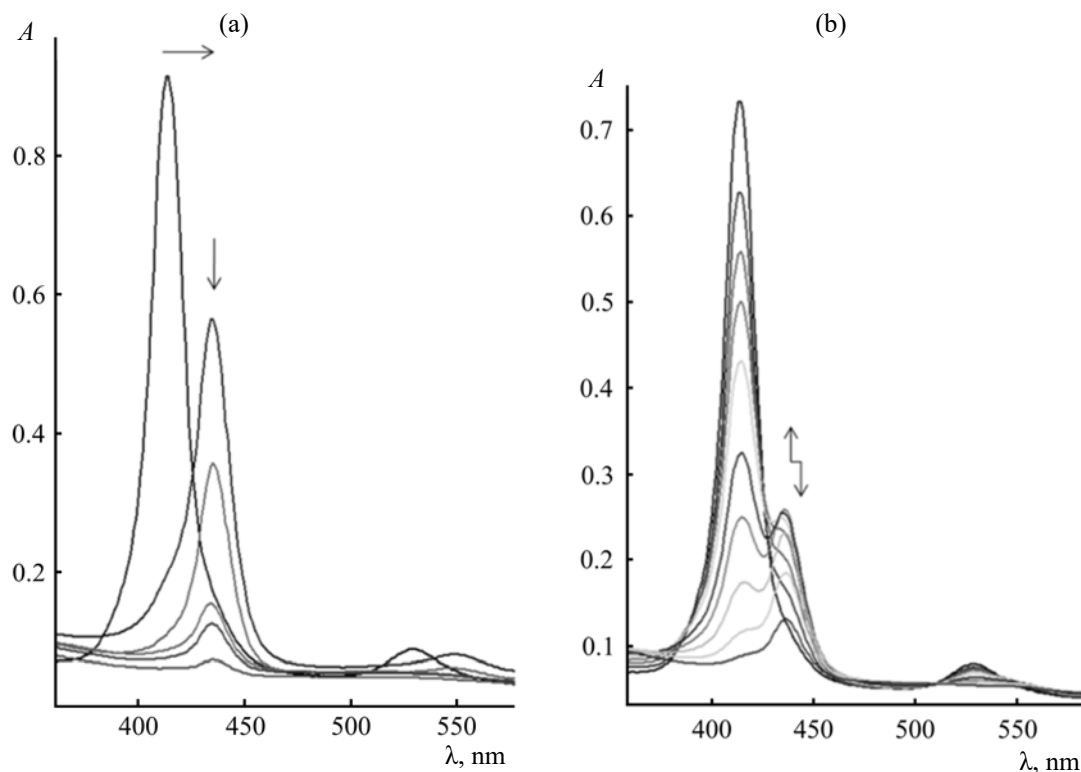
Fig. 2. Changes in the ESP observed with the addition of (a) *tert*-butyl hydroperoxide and (b) di-*tert*-butyl peroxide to the solution of complex **1** in benzene at 298 K.

molecule. The second axial ligand may be the bromine anion or the imidazole or oxygen molecule. The compounds are unstable and are subject to destruction almost immediately as they are formed.

The main peak (100%) in the mass spectra of all the examined Co(III)-tetraphenylporphyrin complexes (regardless of the metal oxidation state and the presence of axial ligands) is the peak of $[M-1]^+$ ion with m/z 671

Table 2. Rate constants[a] of Co-tetraphenylporphyrins **1**, **2a–2c** decomposition in the presence of peroxides in benzene at 298 K

TBP		DBP		TBP		DBP	
$c \times 10^{-4}$, M	$k_{\text{eff}} \times 10^{-4}$, s^{-1}	$c \times 10^{-4}$, M	$k_{\text{eff}} \times 10^{-4}$, s^{-1}	$c \times 10^{-4}$, M	$k_{\text{eff}} \times 10^{-4}$, s^{-1}	$c \times 10^{-4}$, M	$k_{\text{eff}} \times 10^{-4}$, s^{-1}
1				**2b**			
0.19	1.23	2.27		0.77	5.85	0.77	
2.140	2.66	9.07		1.30	8.41	2.28	
17.30	3.73	21.70		21.40	13.60	22.80	
$k_v = 0.0019$ M^{-1} s^{-1}		$k_v = 0.012$ M^{-1} s^{-1}		214.00	27.30	342.00	
2a				$k_v = 0.0069$ M^{-1} s^{-1}		$k_v = 0.0062$ M^{-1} s^{-1}	
0.77	3.33	0.23		**2c**			
1.64	4.10	2.28		11.50	0.14	11.50	0.16
10.80	6.29	22.80		56.10	0.25	56.10	0.27
108.00	10.30	342.00		81.00	0.31	81.00	0.31
$k_v = 0.0029$ M^{-1} s^{-1}		$k_v = 0.003$ M^{-1} s^{-1}		112.00	0.36	112.00	0.37
				k_v, (M^{-1} s^{-1}) = 0.0002		k_v, (M^{-1} s^{-1}) = 0.00018	

[a] k_{eff} and k_v are the effective and true rate constant, respectively.
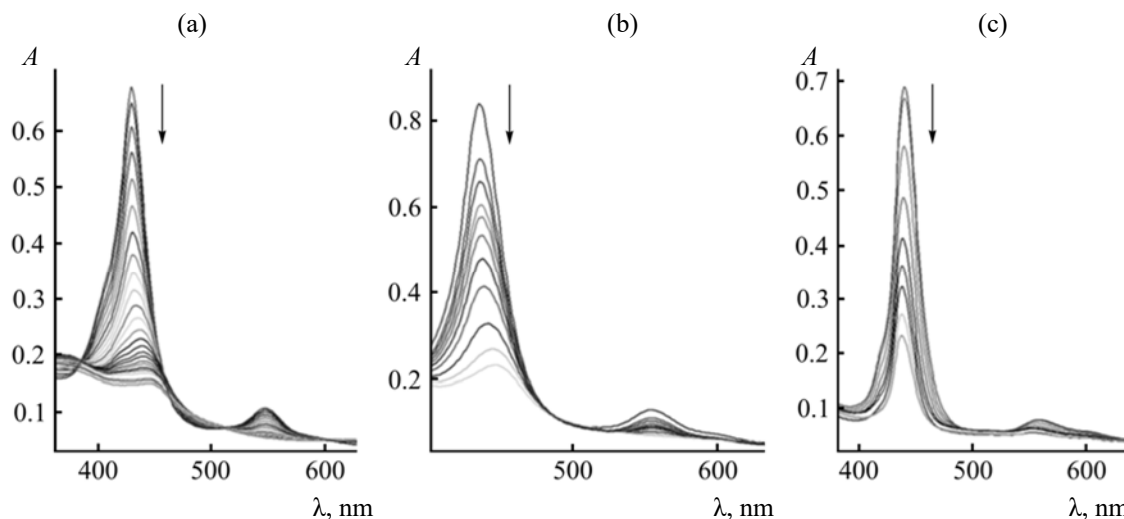
Fig. 3. Changes in the ESP observed with the addition of a solution of *tert*-butyl hydroperoxide to solutions of complexes (a) **2a**, (b) **2b**, and (c) **3c** in benzene at 298 K.

corresponding to the cobalt complex of tetraphenylporphyrin. Porphyrinates containing the Br⁻ acido ligand also have an intense (~50%) peak of $[M + Br]^+$ ion with *m/z* 751 in their spectra.

Analysis of the data presented in [14–19], which concern the decomposition of various metal complexes of 5,10-dimethoxyphenyl tetrabutyltetramethylporphyrin, also confirmes that the first step in the metalloporphyrins interaction with peroxides is the coordination of a peroxide molecule as an axial ligand on the metal cation. According to [14–19] the decomposition rate of different metal complexes of this porphyrin in the presence of peroxide with *tert*-butyl radicals in benzene increases in the series: NiP < Fe(III)P(Ac) < ZnP < Co(III)P(Ac) < Al(III)P(Cl) < MgP, which indicates that the most prone-to-destructtion porphyrinate in the group examined is the Mg complex, which has the highest affinity to oxygen-containing ligands, and the most stable is the Ni complex, which is almost not involved in the additional coordination. The stronger the axial complex MP(ROOR), the more rapid the destruction of porphyrin.

The availability of a free coordination site on a metal cation in the porphyrinate for a peroxide molecule is also a promoter of the macrocycle destruction process. Of the three complexes under study, **3a–3c**, five-coordinated complex **3a**, in which one side of the metalloporphyrin coordination site is available for coordination, exhibits the highest decomposition rate. In **3b**, a peroxide molecule has to compete for the coordination site with a methanol molecule, which leads to an almost twofold slowdown of the porphyrin macrocycle destruction rate. In complex **3c** with two imidazole ligands, the addition of a peroxide molecule to the central cation of the metal is hampered, so that the replacement of at least one imidazole molecule by a peroxide molecule can occur only at high peroxide concentrations and the porphyrinate destruction process lasts several days.

According to [6–11, 33] the destruction of the porphyrin macrocycle (heme catabolism or chlorophyll

Scheme 3.

M = Co(II), Co(III)(Br⁻),
Co(III)(Br⁻)(CH₃OH), Co(III)(Im)₂

3a, **3b**
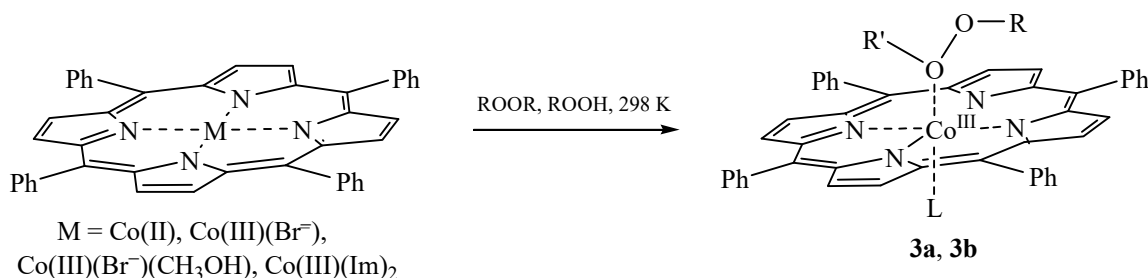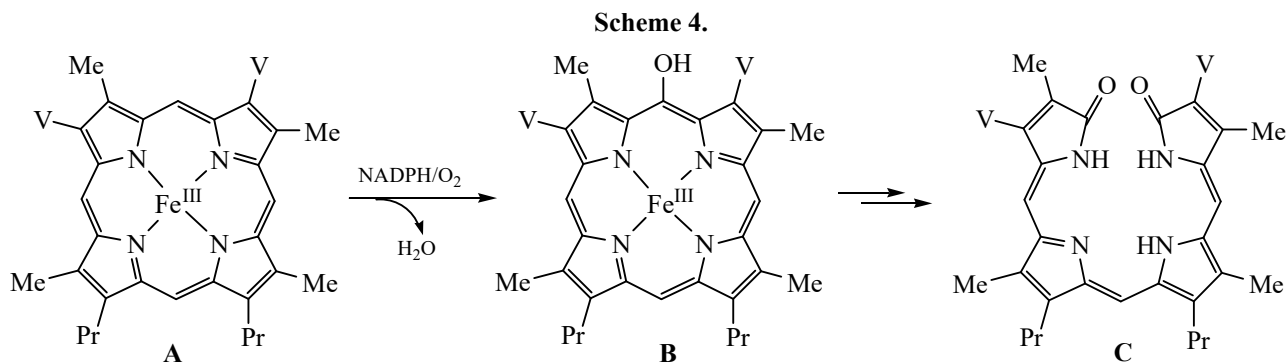
Scheme 4.

Scheme 5.

destruction in plant leaves) begins with the breaking of one methine bridge of the tetrapyrrole macrocycle and the formation of non-cyclic tetrapyrrole (Scheme 4). The process of enzymatic decomposition of blood heme was studied most thoroughly [8–11], according to which the first oxidation step is accompanied by the α-hydroxylation of heme **A**. Subsequently, α-*meso*-hydroxyheme **B** is oxidized to verdoheme and non-cyclic biliverdin **C**.

The mechanism of destruction of chlorophyll molecules, which underlies the plant leaf color change, is much less studied. According to [6, 7], the first step of destruction is dissociation of the Mg complex to the ligand chlorophyll; the second step is breaking of the C–C bond in the *meso*-position of the macrocycle to form a non-cyclic tetrapyrrole (RCC), which is further oxidized to other products (Scheme 5). The thermal destruction of porphyrins, according to [33], also begins with breaking of a –C(R)= bond in the macrocycle.

Analysis of the mass spectra of the products of **3a** reaction with ROOR, in the middle of destruction,

indicates that the destruction of porphyrinates is also likely to begin with the breaking of a macrocycle methine bridge and the formation of non-cyclic tetrapyrrole (*m/z* 608). This non-cyclic tetrapyrrole remains in the metallocomplex form.

It has been found that, unlike the catabolism of natural porphyrins, the destruction of the investigated porphyrinates in the presence of organic peroxides does not stop at the non-cyclic tetrapyrrole formation step. Almost simultaneously with the cleavage of one methine bridge, other methine bridges also undergo successive cleavage, with the formation first of dipyrrole and then monopyrrole compounds. The most intense peak in the mass spectra of the decomposition products of all the porphyrinates studied is the peak corresponding to the unsubstituted pyrrole (*m/z* 66).

The presumed pattern of interaction of Co(III)-tetraphenylporphyrins with peroxide when exposed to light (Scheme 6) comprises a number of basic steps: oxidation of Co(II) to Co(III) under the influence of peroxide; axial coordination of the peroxide on Co(III)-

Scheme 6.

R = H, C(CH$_3$)$_3$.
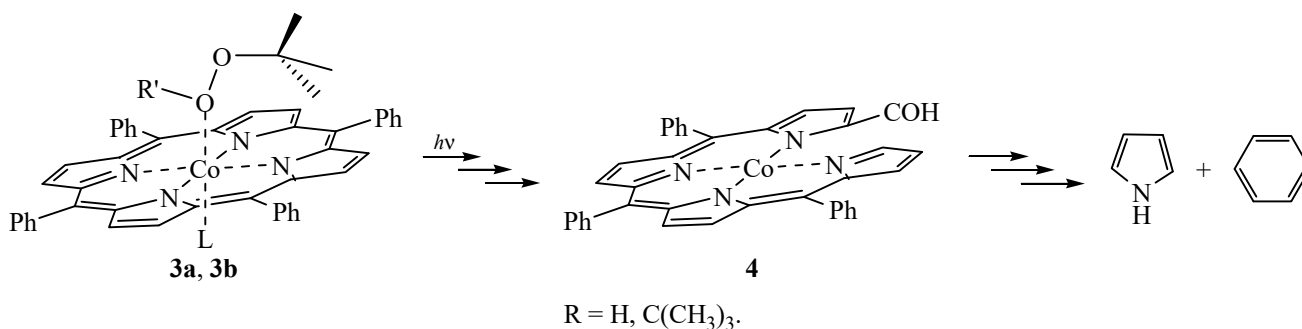
porphyrinate; breaking of a methine bond in the aromatic porphyrin macrocycle and the formation of a non-cyclic tetrapyrrole without loss of the cobalt cation; and further destruction of tetrapyrrole with five- and six-membered heterocycles as final products. Presumably, the destruction of the aromatic porphyrin macrocycle by the first –C(Ph)= bond occurs under the action of the products of homolysis of the peroxide molecule coordinated on the Co(III) cation.

Thus, the study demonstrated that the decomposition rate of Co-tetraphenylporphyrins in the presence of peroxides on exposure to light depends on the cobalt cation valence and on the coordination surrounding (the presence of free coordination sites and the competitive ability of peroxide with respect to available ligands).

A necessary condition for macrocycle destruction in the systems examined is the axial coordination of the peroxide molecule on the porphyrinate metal cation. The blocking of both coordination positions in the cobalt cation in the extracomplex by imidazole molecules prevents the approach of the peroxide molecule to the metal cation of the metalloporphyrin coordination site and increases manyfold the porphyrinate resistance to destruction. The primary product of photochemical destruction of the investigated Co-tetraphenylporphyrins is the Co-complex of open tetrapyrrole. The final products of cobalt-porphyrin decomposition are nitrogen five-membered and six-membered heterocycles.

EXPERIMENTAL

Electron absorption spectra were recorded on a Cary 100 instrument at room temperature (295 K). The ^{1}H NMR spectra were recorded on a Bruker AVANCE-500 instrument (TMS internal reference). The mass spectra were obtained on a Shimadzu Biotech Axima

Confidence Maldi TOF mass spectrometer (dihydroxybenzoic acid matrix). Irradiation of cobalt-porphyrin solutions was carried out using a medium pressure TUNGSRAM 20W F33 mercury lamp.

Co(II)-5,10,15,20-Tetraphenylporphyrin (1). 0.05 g (0.0813 mmol) of tetraphenylporphyrin and 0.144 g (0.813 mmol) of Co(OAc)$_2$ were dissolved in 70 mL of DMF, heated to boiling, boiled for 20 s, and cooled. The filtrate was poured into water, the precipitate was filtered off, washed with water, dried, and chromatographed on alumina using dichloromethane as the eluent [25]. Yield 0.04 g (0.0595 mmol, 72%), R_f 0.77 (1 : 1 hexane–chloroform). IR spectrum, ν, cm^{-1}: 2917, 2849 (CH, Ph), 1694, 1599 (C=C, Ph), 1437 (C=N), 1350 (C–N), 1150, 1073 [δ(C–H, Ph)], 1004 (Co–N), 796 [γ(C–H, pyrrole ring)], 752, 702 [γ(C–H, Ph)], 470 (Co–N). ^{1}H NMR spectrum (CDCl$_3$), δ, ppm: 16.05 br.s (8H, pyrrole), 13.20 br.s (8H, H^o), 8.20 t (8H, H^m, J = 7.7 Hz), 8.01 br.s (4H, H^n). Mass spectrum, m/z (I_{rel}, %): 671.3 (99) [M – H]$^+$ (calculated for C$_{44}$H$_{28}$N$_4$Co: 672). EAS (benzene), $λ_{max}$, nm (logε): 529 (4.16), 413 (5.35). Found, %: C 78.58; H 4.15; N 8.30. C$_{44}$H$_{28}$N$_4$Co. Calculated, %: C 78.69; H 4.20; N 8.34.

Co(III)(Br)CH$_3$OH-5,10,15,20-Tetraphenylporphyrin (2b). 0.3 mL of methanol and 0.4 mL of a bromine solution in chloroform prepared in an amount of 5 drops of bromine per 5 mL of chloroform was added to a solution of complex **1** (0.02 g) in 15 mL of chloroform. The reaction mixture was held at room temperature with stirring for 10 minutes, then evaporated. The residue was recrystallized from methanol. Yield 0.019 g (0.0243 mmol, 83%), R_f 0.69 (1 : 1 hexane–chloroform). ^{1}H NMR spectrum (CDCl$_3$), δ, ppm: 9.18 s (8H, pyrrole), 8.23 d (8H, H^o, J = 7.7 Hz), 7.80–7.76 m (12H, H^{m,n}). Mass spectrum, m/z (I_{rel}, %): 751.1 (55) [M – H –CH$_3$OH]$^+$, 671.3 (100) [M – Br – CH$_3$OH]$^+$ (calculated for C$_{44}$H$_{28}$N$_4$Co:

672). EAS (benzene), λ_{max}, nm (logε): 549 (4.11), 435 (5.37). Found, %: C 66.73; H 3.41; N 7.06. $C_{44}H_{28}N_4BrCoCH_3OH$. Calculated, %: C 67.46; H 3.60; N 7.15.

Co(III)(Br)-5,10,15,20-Tetraphenylporphyrin (2a) was prepared by adding 0.5 mL of a bromine solution (5 drops of bromine per 5 drops of benzene or chloroform) to a solution of compound **1** (0.02 g in 15 mL of benzene or chloroform) and held for several hours. Compound **2a** is stable in solution, but it is partially reduced to complex **1** when recovered from the reaction mixture. ^{1}H NMR spectrum (CDCl$_3$), δ, ppm: 16.05 br.s (8H, pyrrole), 13.20 br.s (8H, H^o), 8.20 t (8H, H^m, J = 7.7 Hz), 8.01 br.s (4H, H^n). Mass spectrum, m/z (I_{rel}, %): 751.1 (60) $[M - H]^+$, 671.1 (97) $[M - Br]^+$ (calculated for $C_{44}H_{28}N_4Co$: 672). EAS (benzene), λ_{max}, nm: 548, 428.

Co(III)(diimidazole)-5,10,15,20-Tetraphenylpor-phyrin (2c). *a*. It was prepared by reacting an air-saturated (non-degassed) solution of porphyrin **1** (0.0013 mg in 20 mL of benzene) with imidazole (0.014 mg) at room temperature.

b. It was prepared by spectrophotometric titration of a solution of complex **2b** (1×10^{-5} M) in benzene with an imidazole solution ($5\cdot10^{-3}$ M). Mass spectrum, m/z (I_{rel}, %): 671.3 (60) $[M - H]^+$, 136 (100) $[2Im]^+$ (calculated for $C_{44}H_{28}N_4Co$: 672). EAS (benzene), λ_{max}, nm (logε): 440 (5.43), 555 (4.13).

The kinetic parameters of the investigated reaction were obtained according to the procedure described in [34]. The effective rate constants (k_{eff}) were determined from the change in the optical density of the solution at working wavelengths (λ 410–418 nm) at definite time intervals using a formally first-order equation (8) with excess of dicumol peroxide and imidazole.

$$k_{eff} = 1/\tau\log(c_0/c_\tau). \qquad (8)$$

Here, c_0 and c_τ are the concentrations of the complex at times 0 and τ, respectively. The values of k_v, k_{eff} and the mean deviation evaluations were optimized using Microsoft Excel and ggh.exe (QB-45) software using the Guggenheim method. The relative error was about 5–10%.

ACKNOWLEDGMENTS

REFERENCES

1. Falk, J., *Porphyrins and Metalloporphyrins*, Amsterdam: Elsevier, 1964.

2. Schmid, R. and McDonagh, A., *The Porphyrins*, New York: Academic Press, 1979, vol. 6.

3. Berezin, B.D., Enikolopyan, N.S., *Metalloporfiriny* (Metalloporphyrins), Moscow: Nauka, 1988.

4. Boyle, R.W. and Dolphin, D., *Photochem. Photobiol.*, 1996, vol. 64, no. 3, p. 469. doi 10.1111/j.1751-1097.1996.tb03093.x

5. O'Connor, A.E., Gallagher, W.M., and Byrne A.T, *Photochem Photobiol.*, 2009, vol. 85, no. 5, p. 1053. doi 10.1111/j.1751-1097.2009.00585.x

6. Moser, S., Müller, T., Oberhuber, M., and Kräutler B., *Eur. J. Org. Chem.*, 2009, no. 1, p. 21. doi 10.1002/ejoc.200800804

7. Müller, T., Rafelsberger, M., Vergeiner, C., and Kräutler, B., *Angew. Chem. Int. Ed.*, 2011, no. 50, p. 10724. doi 10.1002/anie.201103934

8. Montellano, P.R., *Acc. Chem. Res.*, 1998, vol. 31, no. 9, p. 543. doi 10.1021/ar960207q

9. Gozzelino, R., Jeney, V., and Soares, M.P., *Annu. Rev. Pharmacol. Toxicol.*, 2010, no. 50, p. 323. doi 10.1146/annurev.pharmtox.010909.105600

10. Sugishima, M., Sakamoto, H., Higashimoto, Y., Omata, Y., Hayashi, Sh., Noguchi, M., and Fukuyama, K., *J. Biol. Chem.*, 2002, vol. 277, p. 45086. doi 10.1074/jbc.M207267200

11. Sugishima, M., Sakamoto, H., Higashimoto, Y., Noguchi, M., and Fukuyama, K., *J. Biol. Chem.*, 2003, vol. 278, p. 32352. doi 10.1074/jbc.M303682200

12. Lad, L., Schuller, D., Friedman, J., Li, H., Montelano, P.R., and Poulos, T.L., *J. Biol. Chem.*, 2003, vol. 278, p. 7834. doi 10.1074/jbc.M211450200

13. Lissi, E.A., Pizarro, M., Aspee, A., and Romay, C., *Free Radical Biology & Medicine*, 2000, vol. 28, no. 7, p. 1051. doi 10.1016/S0891-5849(00)00193-3

14. Simonova, O.R., Zaitseva, S.V., and Koifman, O.I., *Russ. J. Gen. Chem.*, 2014, vol. 84, no. 1, p. 108. doi 10.1134/S1070363214010174

15. Simonova, O.R., Zaitseva, S.V., and Koifman, O.I., *Russ. J. Gen. Chem.*, 2014, vol. 84, no. 12, p. 2429. doi 10.1134/S1070363214120135

16. Simonova, O.R., Zaitseva, S.V., and Koifman, O.I., *Russ. J. Gen. Chem.*, 2014, vol. 86, no. 6, p. 1322. doi 10.1134/S1070363216060177

17. Simonova, O.R., Zaitseva, S.V., and Koifman, O.I., *Russ. J. Inorg. Chem.*, 2012, vol. 57, no. 6, p. 903. doi 10.1134/S0036023612060204

18. Simonova, O.R., Zaitseva, S.V., and Koifman, O.I., *Russ. J. Inorg. Chem.*, 2013, vol. 58, no. 2, p. 239. doi 10.1134/S003602361302023X

19. Simonova, O.R., Zaitseva, S.V., Zdanovich, S.A., and Koifman, O.I., *Russ. J. Inorg. Chem.*, 2010, vol. 55, no. 6, p. 959. doi 10.1134/S0036023610060215

20. Tovrog, B.S., Diamond, S.E., Mares, F., and Szalkiewicz, A., *J. Am. Chem. Soc.*, 1981, vol. 103, no. 12, p. 3522. doi 10.1021/ja00402a044

21. Steiger, B., Baskin, J.S., Anson, F.C., Zewail, A.H., *Angew. Chem. Int. Ed.*, 2000, vol. 39, no. 1, p. 257. doi 10.1002/(SICI)1521-3773(20000103)39:1<257::AID-ANIE257>3.0.CO;2-3

22. Goodwin, J., Kurtikyan, T., Standard, J., Walsh, R., Zheng, B., Parmley, D., Howard, J., Green, Sh., Mardyukov, A., and Przybyla, D.E., *Inorg. Chem.*, 2005, vol. 44, no. 7, p. 2215. doi 10.1021/ic048701a

23. Trojánek, A., Langmaier, J., Kvapilová, H., Zalis, S., and Samec, Z., *J. Phys. Chem. (A)*, 2014, vol. 118, p. 2018. doi 10.1021/jp500057x

24. Shirazi, A. and Goff, H.M., *Inorg. Chem.*, 1982, vol. 21, no. 9, p. 3420. doi 10.1021/ic00139a030

25. Chizhova, N.V., Kumeev, R.S., and Mamardashvili, N.Zh., *Russ. J. Inorg. Chem.*, 2013, vol. 58, no. 6, p. 740. doi 10.1134/S0036023613060089

26. Walker, F.A., *J. Am. Chem. Soc.*, 1973, vol. 95, no. 4, p. 1150. doi 10.1021/ja00785a025

27. Zhang, Y., Wang, H., and Yang, R.H., *Sensors*, 2007, vol. 7, no. 3, p. 410. doi 10.3390/s7030410

28. Kurtikyan, T.S., Gulyan, G.M., Dalaloyan, A.M., Kidd, B.E., and Goodwin, J., *Inorg. Chem.*, 2010, vol. 49, no. 17, p. 7793. doi 10.1021/ic1007846

29. Goodwin, J., Bailey, R., Pennington, W., Rasberry, R., Green, N., Shacho, S., Yongsavanh, M., Echevarria, V., Tiedeken, J., Brown, CH., Fromm, G., Lyerly, S., Watson, N., Long, A., and Nitto, N., *Inorg. Chem.*, 2001, vol. 40, no. 17, p. 4217. doi 10.1021/ic001442e

30. Sakurai, T., Yamamoto, K., Naito, H., and Nakamoto, N., *Bull. Chem. Soc. Japan*, 1976, vol. 49, no. 11, p. 3042. doi 10.1246/bcsj.49.3042

31. Ziyadova, T.M., Burmistrov, V.A., Semeikin, A.S., and Koifman, O.I., *Macroheterocycles*, 2015, no. 8(3), p. 274. doi 10.6060/mhc1409262

32. Yamada, T. and Kamiya, Y., *Bull. Chem. Sic. Japan*, 1980, vol. 53, no. 4, p. 1077. doi 10.1246/bcsj.53.1077

33. Antina, E.V., Balantseva, E.V., and Berezin, M.B., *Russ. J. Gen. Chem.*, 2011, vol. 81, no. 6, p. 1222. doi 10.1134/S1070363211060260

34. *Eksperimental'nye metody khimicheskoi kinetiki* (Experimental Methods of Chemical Kinetics), Emanuel', N.M. and Sergeev, G.B., Eds., Moscow: Vysshaya Shkola, 1980.